CYCLIC FATIGUE TESTING OF SURFACE-MICROMACHINED THERMAL ACTUATORS

Robert A. Conant and Richard S. Muller, Berkeley Sensor & Actuator Center,
Department of EECS, University of California, Berkeley, 94720-1770

ABSTRACT

Long-term testing of surface-micromachined *U*-shaped thermal actuators has been carried out. Actuators operated at power levels lower than 8 mW (12 µm of displacement) operated satisfactorily for more than 100 million cycles at 660 Hz, with a failure defined as the point at which the displacement decreases by 20%. Plastic deformation had been observed in actuators operated above 8 mW, and the plastic deformation has been shown to be associated with the high temperatures encountered during operation. The failure rate of the actuators is dependent on the total time the actuators are at the elevated temperatures encountered during operation, rather than on the number of actuation cycles. This paper provides a guide for MEMS designers that shows the lifetime of a thermal actuator as a function of its drive power.

INTRODUCTION

Products from automobiles to CMOS circuits require extensive reliability testing throughout their development and manufacturing processes. As MEMS move from the universities – where "if one device fails we simply use another" – to commercial products, where reliability is paramount, the long-term reliability of every MEMS building block must be well characterized. Thermal actuators are attractive for many MEMS applications because of the possibility of positioning using CMOS-compatible voltages and currents. Thus far, however, only anecdotal data have been published to document the failure modes of surface-micromachined thermal actuators and to validate their use by long-term reliability testing[2].

Thermal actuators have inherent limitations for long-term use because, at high temperatures, polycrystalline silicon can lose the nearly perfect linear-elastic properties that makes the material so attractive for MEMS. In fact, polysilicon can deform plastically at the high temperatures encountered during the operation of some thermal actuators. However, if operated at sufficiently low temperatures, thermal actuators appear to be very reliable. Comtois has seen plastic deformation in thermal actuators heated for a few seconds (a phenomenon that he has demonstrated to cause an increased actuator force). Comtois calls this effect "back bending".[3] Plastic deformation, however, is not usually beneficial. Long-term positioning accuracy becomes impossible when there is significant plastic deformation; therefore, the long-term wear characteristics of thermal actuators must be studied to qualify these actuators for use in commercial products.

MICROMACHINED *U*-SHAPED THERMAL ACTUATORS

We have carried out experiments on micromachined *U*-shaped thermal actuators, as shown in Figure 1. The actuators were fabricated in the UC Berkeley Microlab in a process similar to that offered by MCNC for MUMPS. The actuators were fabricated from 2-µm thick polysilicon above a 2-µm thick layer of sacrificial oxide. Similar actuators have been characterized previously[1] and used for various MEMS applications[2,3,4].

The *U*-shaped actuator converts electrical to mechanical energy through ohmic heating and the thermal expansion of polysilicon. Applying a voltage to the actuator causes more resistive heating in the hot than in the cold arm due to the higher current density in the hot arm. As the hot-arm temperature increases the arm extends, and this extension causes lateral motion of the actuator tip. Figure 2 shows a plot of the actuator displacement as a function of the drive power.

Thermal actuators have some advantages over other microactuation methods: they provide fairly large forces (on the order of a few micro-Newtons) and large displacements (greater than 16 µm) at CMOS compatible voltages and currents. The main disadvantage of thermal actuators is their large power consumption -- at full displacement, our actuators required approximately 22 mW.

The power is dissipated through two dominant paths: heat conduction through the polysilicon to the substrate through the contacts, and heat conduction to the substrate through the 2 µm air gap below the actuator. Convection around the hot arm contributes a small amount of cooling, but rough calculations indicate that convection plays a much smaller role than does heat conduction in the thermal actuator. Radiation, although it can be visible to the naked eye at large power levels, dissipates less than 2% of the total power at the highest temperatures used. When driven above roughly 1.5 kHz, the thermal actuators are not able to cool down to the substrate temperature and the actuator displacement decreases. The actuators operate at full deflection up to 1.3 kHz, which implies that cooling is essentially completed within about 0.4 ms.

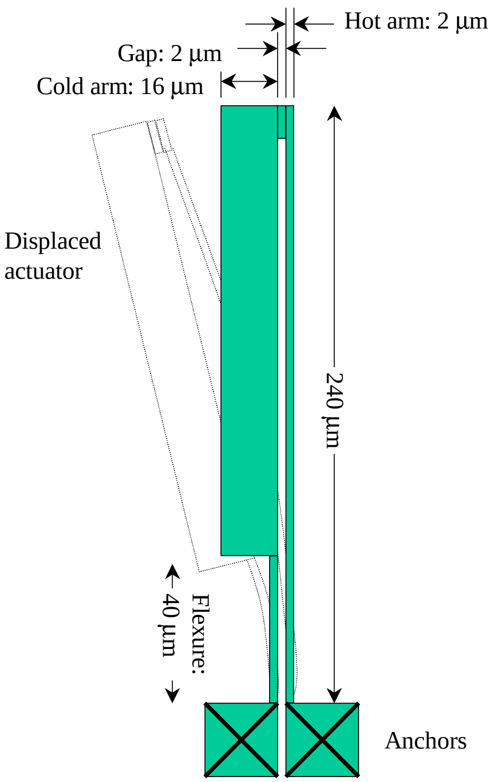

Figure 1: Schematic of a micromachined thermal actuator. The hot arm is 240 x 2 mm, the cold arm is 15 x 200 mm, and the flexure is 40 x 2 mm. The hot arm is separated from the cold arm and the flexure by a 2 mm gap.

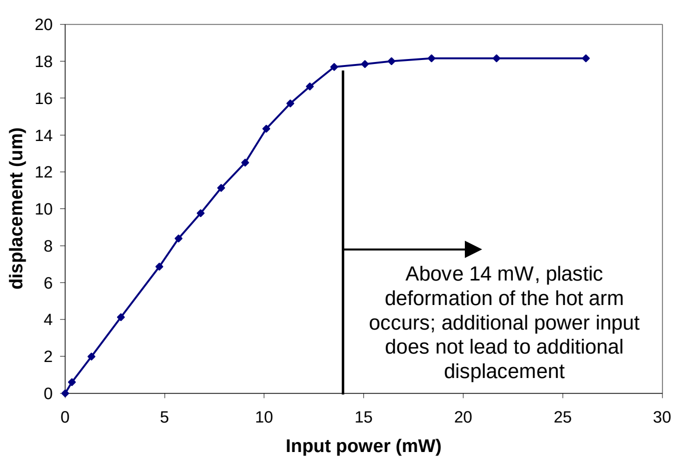

Figure 2: Displacement versus input power for a thermal actuator.

TESTING

In order to determine the long-term reliability of micromachined thermal actuators, we used periodic drive voltages and measured the displacement characteristics throughout each actuator lifetime. The test setup (a schematic of which is shown in Figure 3) consists of a pulse generator, thermal actuators, a microscope, and a camera attached to a computer for data acquisition and analysis. The function generator applied a square wave at 660 Hz. The actuators cool completely in 0.4 ms; therefore, the 660 Hz drive function provides quasi-steady-state operation of the actuators.

At periodic intervals, the computer, camera, and microscope were used to record an image of each actuator. Since the actuators were operated at 660 Hz – a much higher frequency than the video frequency (30 Hz) – the images show a superposition of the rest position of the actuator (where 0 Volts is applied), and the displaced position (with a nonzero applied voltage). Figure 4a shows an actuator before testing, and Figure 4b shows a sample actuated with a square wave drive signal providing 11.1 mW of drive power when the drive waveform is high, and 0 mW when the drive waveform is low. The second image (b) shows the superposition of the actuator in the rest and the displaced positions. Figure 4c shows the "best-fit" displacement for the actuator; the rest position has moved to -2 µm, and the displaced position is +7 µm. The actuator is permanently deformed – the rest position (with no voltage applied) has moved 2 µm, and the actuator position with 11.1 mW of applied power has changed from +15.3 µm down to +7 µm. The total displacement has reduced from 15.3 µm to 9 µm – a reduction of 41%.

This method of measuring the position offset was used on each actuator over its lifetime, and the resulting data were used to characterize thermal actuator wear.

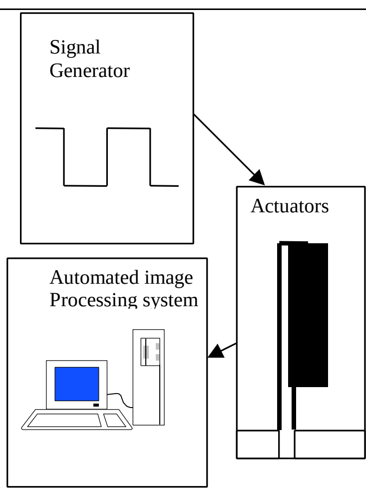

Figure 3: Test setup for long-term testing of thermal actuators. A signal generator provides a square wave (1-20 V amplitude at arbitrary frequency); automated image-processing system analyzes the deformation and maximum displacement behavior *versus* time.

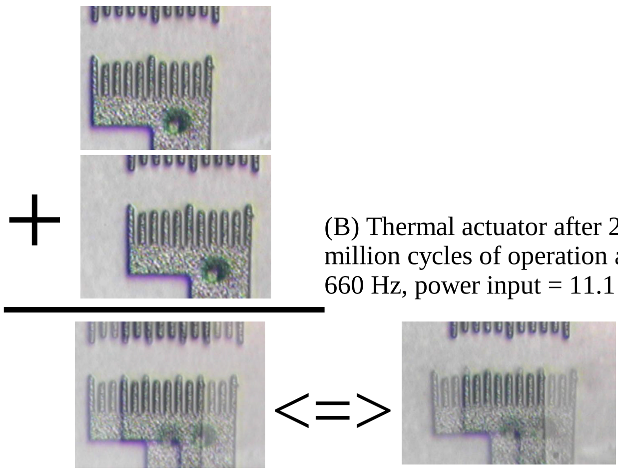

Rest and actuated position is determined by comparing the displaced image to the image before actuaton. This schematic shows that superposing two offset images of the initial image can be used to fit the measured displacement. The error due to the angle of the displaced actuator was eliminated by looking at one row of the image rather than the entire image.

Figure 4. Schematic of image processing algorithm used to determine actuator displacement. The inset images show the tip of a thermal actuator with a verneer used to measure displacement.

RESULTS

Figure 5 shows a typical plot of the displacement of two actuators versus the number of cycles (both actuators were operated at 660 Hz). The actuator operated at 7.5 mW shows an initial displacement of 12.0 μm, and very little change in total displacement with time. The actuator operated at 11.1 mW shows an initial displacement of 15.3 μm; however, its performance degrades over time to reach 7.1 μm displacement after 14.5 million cycles. Since the failure of these thermal actuators is progressive rather than catastrophic (as shown by the slow change in actuator characteristics over 14.5 million cycles), we chose the failure threshold as the time when the actuator displacement is less than 80% of the initial displacement.

Using this threshold failure criterion, the high-power actuator failed after 2 million cycles from plastic deformation of the hot arm. Figure 5 shows a photomicrograph of this actuator after 14.5 million cycles. Notice the permanent deformation of the hot arm with no voltage applied. The actuator operated at 7.5 mW, however, shows less than 10% change in displacement after 100 million cycles.

Figure 6 shows the measured lifetime of five different actuators versus power and displacement. The actuators operated at 7.5 mW and 6.8 mW had not failed after 100 million cycles, while those actuators operated above 8 mW had failed. The line on the chart shows the expected lifetime of thermal actuators versus drive power (the lower axis) and displacement (the upper axis). This graph can be used as a guide for designers to determine the maximum power level for a given lifetime.

Plastic deformation

At high power levels, thermal actuators get sufficiently hot to emit visible radiation, and the temperature of the actuator hot arm rises above the brittle-to-ductile transition (which is approximately 660°C[6]). When an actuator is operated at temperatures above the brittle-to-ductile transition temperature, the stress in the hot arm causes plastic deformation and the rest position of the actuator changes. When the drive voltage is removed, the actuator moves to a negative displacement position. This "backbending" has been noted in the literature, and has been utilized to provide larger output forces of thermal actuators.

The location of the plastic deformation occurs at the point of highest temperature in the actuator, *not* at the position of highest stress. A first-order finite-element model (neglecting the effects of temperature on thermal conductivity, resistance, and the coefficient of thermal expansion) was used to get an estimate of the relative stress and temperature distributions in the thermal actuator. Figure 7 shows the relative temperature distribution in the structure -- the highest temperature is in the hot arm, as expected. The maximum stress, however, occurs at the joint between the flexure and the cold arm – *not* in the hot arm. Since there is significant plastic deformation in the hot arm where the temperature is highest, and no visible plastic deformation of the flexure where the stress is highest, it is evident that the high temperature of the hot arm facilitates the plastic deformation.

The plastic deformation of thermal actuators operated at 660 Hz (50% duty cycle) are almost identical to actuators operated at 66 Hz (50% duty cycle) for the same amount of *time* – not the same number of cycles. This implies that the wear of the thermal actuators is more closely related to the amount of time the actuators are held at the elevated temperatures encountered during operation, rather than to the number of cycles. For example, actuators driven at 16 mW, 60 Hz for 2 minutes show the same deformation as actuators driven at 16 mW, 660 Hz for 2 minutes since both are subjected to the elevated temperature for the same amount of time.

Substrate/Actuator Adhesion

Actuators operated above a silicon nitride layer (rather than a conducting polysilicon layer) failed by adhering to the underlying material. The actuator adhesion is related to the voltage at which the actuator is driven (not its power level), and the underlying material composition. Four different combinations of resistances and underlying materials were tested: 8.43 kΩ and 1.94 kΩ actuators above a polysilicon ground plane and above silicon nitride. The two actuators of different resistance were made in the same fabrication process, except the lower resistance actuators were annealed longer, resulting in a higher dopant concentration and, therefore, a lower resistance.

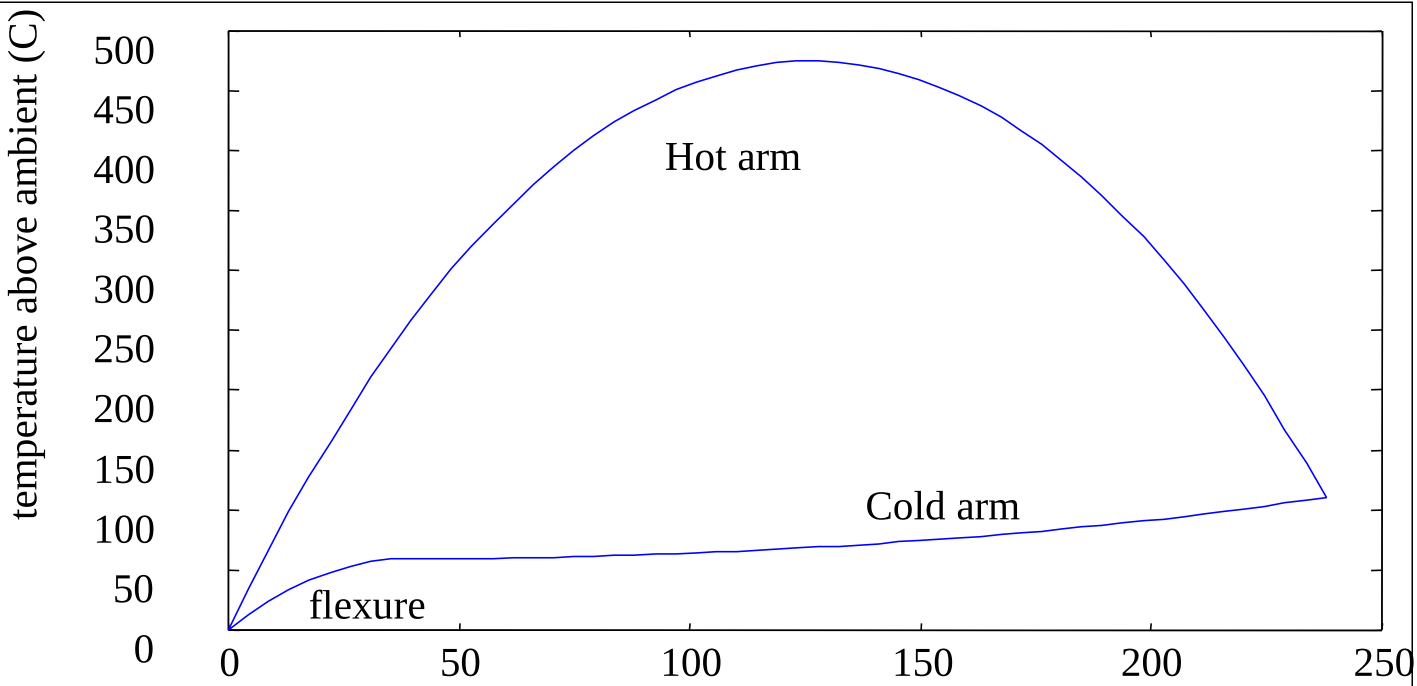

Figure 7: Simplified finite-element model results showing temperature distribution in the thermal actuator.

The factor-of-four difference in the resistance of the actuators gives a factor-of-two difference in voltage for the same power level. The higher resistance actuators above silicon nitride all failed by adhesion before 24 hours of operation at 66 Hz, regardless of the applied power level. The lower resistance actuators, however, lasted significantly longer. Operated at the same 66 Hz above the silicon nitride, the actuators operated at low power lasted more than 5 days; however, they too eventually adhered to the silicon nitride. This adhesion of the polysilicon actuators to the silicon nitride substrate appears to be a function of the lab humidity. However, we have not identified any significant advantage to operating thermal actuators above a non-conducting material layer, so experiments to further characterize the adhesion between the polysilicon thermal actuators and the silicon substrate have not been performed.

CONCLUSIONS

Surface-micromachined *U*-shaped thermal actuators operated at levels below 8 mW appear to be very reliable; there is less than 20% change in these actuator displacements after 100 million cycles. Long-term use of these actuators in stepping configurations, where the actuators must provide some minimum displacement but not accurate positioning, is possible. However, because the displacement characteristics of these actuators change over time, precise positioning using thermal actuators is possible only in closed-loop systems.

REFERENCES

1. Bright, V.M., J.H. Comtois, J.R. Reid, D.E. Sene, "Surface micromachined micro-opto-electro-mechanical systems," *IEEE Transactions on Electronics*, Feb 1997, vol E80-C (no 2): 206-213.

2. Comtois, J. H., M. Adrian Michalicek, and Carole Craig Barron, TRASDUCERS '97 Int'l Conf. On Solid State Sensors and Actuators, June 16-18, 1997, Chicago, IL, pp 769-772

3. Comtois, J. H., and V. M. Bright, "Surface Micromachined Polysilicon Thermal Actuator Arrays and Applications," *Solid State Sensor and Actuator Workshop*, Hilton Head, South Carolina, USA, 1996, pp. 174-177.

4. Field, L., D. Buriesci, P. Robrish, and R. Ruby, "Micromachined 1x2 Optical Fiber Switch," *Proc. Transducers '95/Eurosensors IX*, Stockholm, Sweden, 1995, pp. 344-347.

5. Gunawan, D., L. Lin, and K. Pister, "Micromachined Corner Cube Reflectors as a Communication Link," *Sensors and Actuators A*, 46-47, pp. 580-583, 1995.

6. Rybicki, G.C. and P. Pirouz, *Indentation Plasticity and Fracture in Silicon*, 1988, NASA Technical Paper 2863.

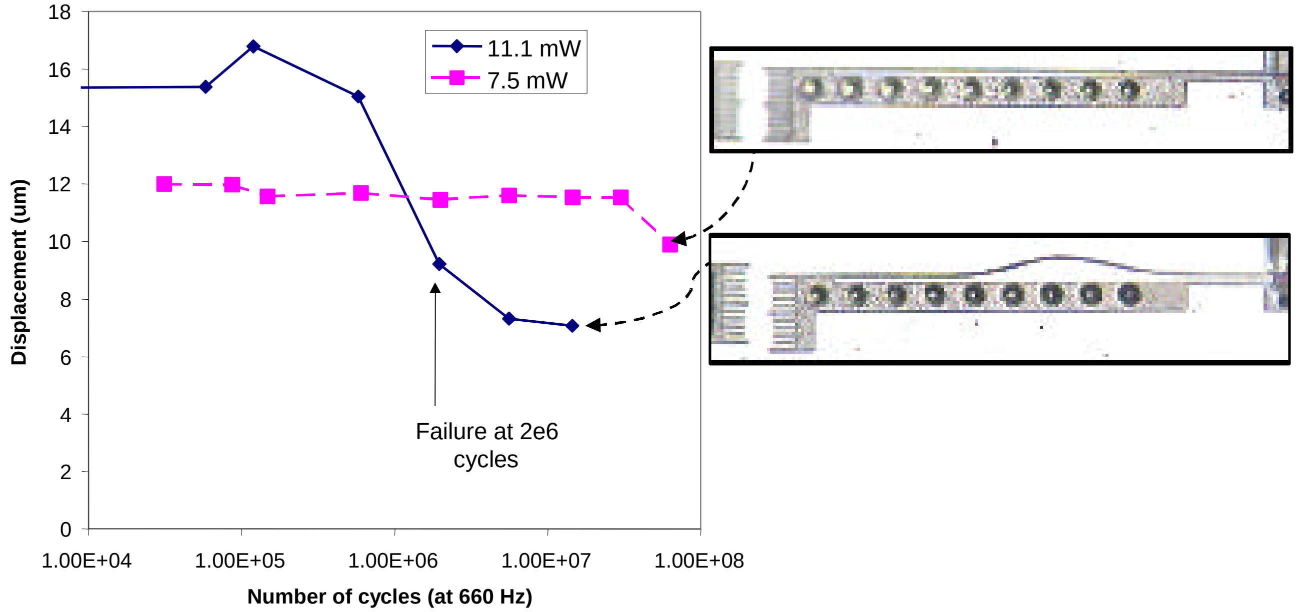

Figure 5: Displacement versus number of cycles for two thermal actuators. The inset images show the permanent displacement of the actuator operated at 11.1 mW after 4.5 million cycles. The actuator operated at 7.5 mW shows very little permanent displacement after 4.5 million cycles.

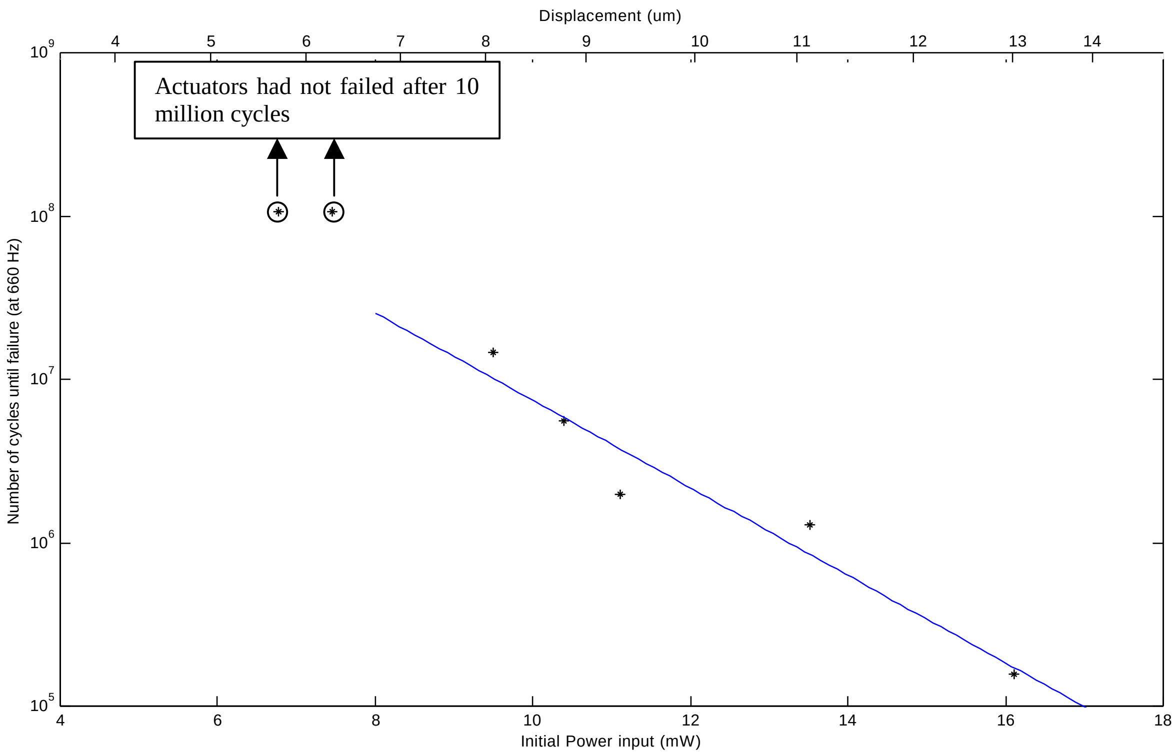

Figure 6: Lifetime of thermal actuators at different power levels. The actuator drive power in the "on" state, plotted on the bottom axis, corresponds to the displacement shown on the top axis. The line on the chart shows the best-fit line that can be used to estimate actuator lifetime.